Quantum entanglement in the multicritical disordered Ising model

István A. Kovács *

Department of Physics and Astronomy, Northwestern University, Evanston, Illinois 60208, USA;
Northwestern Institute on Complex Systems, Northwestern University, Evanston, Illinois 60208, USA;
and Department of Engineering Sciences and Applied Mathematics, Northwestern University, Evanston, Illinois 60208, USA

(Received 22 April 2024; accepted 27 May 2024; published 6 June 2024)

Quantum entanglement at critical points is often marked by universal characteristics. Here, the entanglement entropy is calculated at the quantum multicritical point of the random transverse-field Ising model (RTIM). We use an efficient implementation of the strong disorder renormalization group method in two and three dimensions for two types of disorder. For cubic subsystems we find a universal logarithmic corner contribution to the area law $b\ln(\ell)$ that is independent of the form of disorder. Our results agree qualitatively with those at the quantum critical points of the RTIM, but with new b prefactors due to having both geometric and quantum fluctuations at play. By studying the vicinity of the multicritical point, we demonstrate that the corner contribution serves as an "entanglement susceptibility," a useful tool to locate the phase transition and to measure the correlation length critical exponents.

DOI: 10.1103/PhysRevB.109.214202

I. INTRODUCTION

Quantum critical points (QCPs) occur in the ground state of quantum systems by tuning a quantum control parameter that governs quantum fluctuations. Quantum multicritical points (QMCPs) emerge at the junction of two or more quantum phase transitions, resulting in novel universality classes [1]. While QCPs have been well characterized theoretically, our understanding of QMCPs remains much more limited. From an experimental perspective, QMCPs are expected to be less elusive to study than QCPs [2–5] (see, for example, the recent experimental work on the ferromagnetic QMCP in the disordered compound $Nb_{1-y}F_{2+y}$ [6]). On the theoretical side, our recent study showed that the QMCP of the ferromagnetic random transverse-field Ising model (RTIM) exhibits ultraslow, activated dynamic scaling [7], governed by an infinite disorder fixed point (IDFP) [8,9]. The dominant role of disorder ensures that the applied strong disorder renormalization group (SDRG) method [10,11] is asymptotically exact [9,12–15], meaning that the obtained numerical results approach the exact results at large scales.

In this paper, our goal is to quantify the universal aspects of quantum entanglement at the QMCP of the RTIM. Our results contribute to a better understanding of the universal properties of quantum many-body systems in the vicinity of quantum phase transitions [16–19]. We consider the ground state of the system, $|\Psi\rangle$, and measure the entanglement between a subsystem A and the rest of the system B by the von Neumann entropy of the reduced density matrix $\rho_A = \mathrm{Tr}_B|\Psi\rangle\langle\Psi|$ as

$$\mathcal{S}_A = -\mathrm{Tr}_A(\rho_A \log_2 \rho_A). \tag{1}$$

Known as the "area law" [18], $\mathcal{S}$ is generally expected to scale with the area of the interface separating $\mathcal{A}$ and $\mathcal{B}$ in the ground state. At QCPs, however, there are often additional universal corrections, which can be dominant in one-dimensional systems [20–22]. In higher dimensions it is much more challenging to study quantum entanglement in interacting systems. At the QCP of two-dimensional interacting systems there are additional logarithmic terms, which are expected to be universal, as demonstrated for multiple models, including the transverse-field Ising model [23], the antiferromagnetic Heisenberg model [24], and the quantum dimer model [25,26].

Disordered systems have been also extensively studied, with the RTIM as a prominent example [27], as at an IDFP disorder fluctuations dominate over quantum fluctuations, simplifying the analytic and numerical treatment [28–34]. In addition to critical exponents, the SDRG method also offers an efficient way to calculate the entanglement properties [35]. While the area law is again found to be valid in disordered magnets, the total entanglement entropy is not universal and not extremal at the critical point in higher dimensions. Yet, in the RTIM there is a singular, logarithmic corner contribution to the entanglement entropy that is universal and extremal at the critical point, as shown in $d = 2$, 3, and 4 [35].

In this paper, we show that the same kind of scenario holds at the so far uncharted QMCP of the RTIM in two and three dimensions. As our main result, we quantify the logarithmic corner contribution to the entanglement entropy of cubic subsystems with high precision and show that it is universal, i.e., independent of the form of disorder. In addition, we show that just as at the QCP of the RTIM [35], the corner contribution serves as an "entanglement susceptibility," determining the location of the QMCP as well as the correlation length critical exponents [36].

*Contact author: istvan.kovacs@northwestern.edu

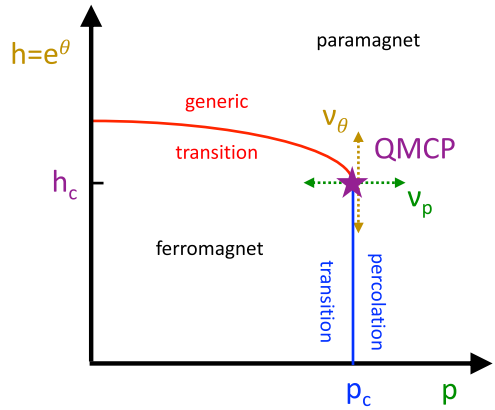

FIG. 1. Phase diagram of the RTIM in two and higher dimensions. The QMCP (purple) emerges at the junction of the percolation transition at the bond dilution parameter $p = p_c$ (blue line) and the generic disordered universality class (red), when the h magnetic field is tuned to its critical value. Deviations from the QMCP are governed by two correlation length exponents, ν_θ and ν_p, corresponding to the two control parameters.

II. MODEL AND METHODS

The Hamiltonian of the RTIM can be expressed as

$$\mathcal{H} = -\sum_{\langle ij \rangle} J_{ij}\sigma_i^x\sigma_j^x - \sum_i h_i\sigma_i^z, \tag{2}$$

where the $\sigma_i^{x,z}$ Pauli matrices represent spins at sites i of a d-dimensional cubic lattice. The spins interact through the J_{ij} nearest-neighbor couplings, and are exposed to the h_i transverse fields. Both the couplings and the fields are non-negative random numbers, drawn from some distributions. To test the universality of the results we will use two different types of disorder as in Refs. [7,28,34,35]. For both types of disorder, the couplings are uniformly distributed in the interval (0,1]. The transverse fields are either constant $h_i = h$, $\forall i$ (*fixed-h* disorder), or are drawn independently from the interval $(0, h]$ (*box-h* disorder). The choice of fixed-h disorder can be motivated by experimental realizations of the model where the transverse field is homogeneous, e.g. in $LiHo_xY_{1-x}F_4$ [37].

Just as for the QCP, the QMCP of the RTIM is studied with the quantum control parameter given by the logarithmic variable $\theta = \ln(h)$ [28,34,35]. To arrive at the QMCP, the bond percolation probability p must be tuned to its critical value p_c, as illustrated in Fig. 1. For sufficiently small fields, we observe a quantum phase transition dictated by the classical percolation transition of the lattice [38,39]. This percolation line ends at the QMCP, where it meets the line of the generic QCP transition. Along the generic transition line the critical behavior falls in the same universality class as the undiluted ($p = 0$) system [28,34,35]. At the QMCP a new universality class emerges, characterized by a new set of critical exponents, due to the interplay of both geometric and quantum fluctuations (see Ref. [7] and Table I).

The SDRG method offers a very efficient way to obtain the ground state of the RTIM [28,34] by iteratively creating an effective description of the ground state and low-energy excitations. At each decimation step of the process the largest local term in the Hamiltonian in Eq. (2) is eliminated. There are two options: The largest term could either be the strongest J coupling or the largest h transverse field in the system. Second-order perturbation theory then dictates the emergence of new, weak couplings depending on the two options as follows. *J decimation:* When the largest term in the system is a coupling, J_{ij}, the two connected spins tend to be aligned at low energies and can be merged into an effective spin cluster of the joint moment, $\tilde{\mu} = \mu_i + \mu_j$. This effective spin is then placed in an effective transverse field, $\tilde{h} = h_i h_j / J_{ij}$. *h decimation:* When the largest term in the system is a transverse field, h_i, the spin does not contribute to the magnetic properties of the system at low energies and can be eliminated. However, new weak effective couplings need to be placed between each pair of neighboring spins, j and k, $\tilde{J}_{jk} = J_{ji}J_{ik}/h_i$. In the case when a coupling is generated between a pair of spins that are already interacting by another coupling, the maximum of the two J couplings is taken. This choice is known as the *maximum rule*, which is known to be a valid approximation at an IDFP where the distribution of the couplings becomes extremely broad. Note that as a result, in all cases, the new effective terms are smaller than the eliminated terms. At each successive step of the SDRG, another spin is eliminated as the energy scale is

TABLE I. Critical and multicritical properties of the RTIM: The universal b prefactors of the corner contribution to the entanglement entropy at the QMCP are indicated in bold. "f" stands for fixed-h disorder, while "b" indicates box-h disorder. The results of this work are indicated in bold. NA=not available.

		Percolation QCP [33,42,43]	Generic QCP [35]	QMCP [7]	
$d = 2$	p_c or θ_c	0.5 bond	−0.17034(2) f	−0.481(1) f	
		0.592746 site	1.6784(1) b	0.783(1) b	
	ν_θ	NA	1.24(2)	1.382(7)	
	ν_p	4/3–1.333	NA	1.168(10)	
	$b^{(2)}$	$-\frac{5\sqrt{3}}{36\pi} \approx -0.07657$	−0.029(1)	**−0.0684(4)**	
$d = 3$	p_c or θ_c	0.248812 bond	−0.07627(2) f	−0.5055(10) f	
		0.311608 site	2.5305(10) b	0.770(1) b	
	ν_θ	NA	0.98(2)	1.123(10)	
	ν_p	0.8762(12)	NA	0.86(1)	
	$b^{(3)}$	1.72(3)	0.012(2)	**0.155(10)**	

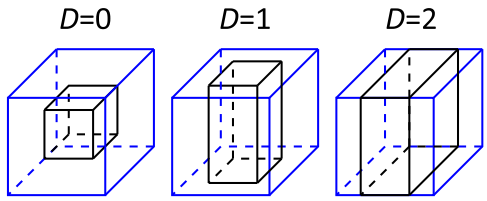

FIG. 2. Subsystem shapes used in the geometric method in $d = 3$ [35]. Each subsystem spans the full L length in D directions, with a size of $\ell = L/2$ in the remaining directions. With periodic boundary conditions, the corner contribution is only present for the cubic subsystem, $D = 0$.

continuously lowered, until all degrees of freedom have been decimated out. In practice, the most efficient implementation of the SDRG method works in a parallel manner [28], relying on graph algorithms to obtain the same results as the above-mentioned conceptual picture, but in nearly linear time as a function of the number of spins. The ground state of the RTIM is then obtained as a collection of independent ferromagnetic clusters of various sizes—created at each h-decimation step. In each cluster, all spins point in the same directions as all others, known as a Greenberger-Horne-Zeilinger (GHZ) state $\frac{1}{\sqrt{2}}(|\uparrow\uparrow\cdots\uparrow\rangle + |\downarrow\downarrow\cdots\downarrow\rangle)$.

While the emerging clusters are generally fractal-like disconnected objects [35,40], each contributes equally to the entanglement entropy of a subsystem, as long as it is intersected by the subsystem in a way that there are some site(s) inside and outside [41]. With the definition in Eq. (1) each such intersected cluster contributes to the amount of $\log_2 2 = 1$, turning the calculation of the entanglement entropy into a cluster counting task.

Interestingly, the entanglement entropy depends sensitively on the shape of the subsystem. As shown at the percolation [36,42] and generic [35] QCPs, subsystems with sharp corners lead to universal corner contributions. For example, a cubic subsystem in $d = 3$ is expected to yield the critical result of

$$\mathcal{S}^{(3)}(\ell) = a_2\ell^2 + a_1\ell + \mathcal{S}^{(3)}_{\rm cr} + O(1) \tag{3}$$

in the limit of large system sizes $1/L \to \infty$ when the ℓ linear size of the subsystem is proportional to the system size. Here, $\mathcal{S}^{(3)}_{\rm cr} = b^{(3)}\ln(\ell) + O(1)$, and only the $b^{(3)}$ prefactor is universal [35], with the values summarized in Table I. Outside the critical point, the finite correlation length is expected to lead to a finite corner contribution, as we will discuss later. Form this form it is apparent that the corner contribution is relatively small compared to the nonuniversal terms. Yet, it can be measured directly to high precision using the so-called *geometric method* [35,36], at least in the case of periodic boundary conditions applied here. The idea is to use additional measurements that have a different shape, fully spanning the system in D dimensions, incorporating a different amount of each term seen for a cubic subsystem due to a different amount of surface elements, such as corners, edges, and facets. In $d = 3$, in addition to cubes, we also consider columns ($D = 1$, has edges, but no corners) and slabs ($D = 2$, no edges, and no corners), as illustrated in Fig. 2. More generally, in d dimensions, we considered d different geometries with $D = 0, 1, \ldots, d-1$ to obtain the corner contribution [35] as

$$\mathcal{S}^{(d)}_{\rm cr} = \sum_{D=0}^{d-1}\left(-\frac{1}{2}\right)^D\binom{d}{D}\mathcal{S}^{(d)}_D. \tag{4}$$

Note that the geometric method cancels out all other terms, not only on average over samples, but exactly in each sample even at small sizes, where there are additional finite-size effects contributing to the asymptotic terms. Hence, the geometric method often provides high-precision results with relatively small finite-size effects.

III. RESULTS

The locations of the QCPs and QMCP are known to high precision, as listed in Table I. Here, we also list the relevant critical and multicritical exponents, all of which are known to be universal, i.e., randomness independent [7]. The known b values of the corner contribution to the entanglement entropy are also listed here for $d = 2, 3$ at the percolation and generic QCPs. We study large systems up to a linear size of $L = 2048$ in $d = 2$ and $L = 64$ in $d = 3$. The number of realizations used in the numerical calculations at the QMCP is typically 100 000, apart from the largest sizes, where we have at least 50 000 samples. The total computational effort exceeded 10 CPU years.

We implemented the "geometric method" to obtain the corner contribution as well as the other prefactors a_i in Eq. (3). As expected, the area law is found to be valid at the QMCP, with nonuniversal a_i prefactors. In $d = 2$, $a_1 = 0.237(1)$ for box-h disorder and $a_1 = 0.662(1)$ for fixed-h disorder. In $d = 3$, $a_2 = 0.163(1)$ and $a_1 = -0.11(1)$ for box-h disorder, with $a_2 = 0.546(1)$ and $a_1 = -0.24(1)$ for fixed-h disorder.

At the QMCP, we see clear evidence of a logarithmic corner contribution in both $d = 2$ and $d = 3$, as shown in Fig. 3, with the insets indicating the two-point fits of $b^{(d)}$ from consecutive sizes. As a clear sign of universality, the extrapolated $b^{(d)}$ values are found to be disorder independent, and are listed in Table I. In both two and three dimensions, the $b^{(d)}$ prefactors are between those at the generic and percolation QCPs.

While the entanglement entropy is not extremal at higher-dimensional QCPs or at the QMCP, the corner contribution is only present at the phase transitions, suggesting an extremal $\mathcal{S}^{(d)}_{\rm cr}$ as a function of either $\delta_\theta = \theta - \theta_c$ or $\delta_p = p - p_c$. For $\delta > 0$ we arrive at the paramagnetic Griffiths phase, while $p - p_c < 0$ leads to a ferromagnetic Griffiths phase. Note that along the $p = p_c$ critical line for $\theta < \theta_c$, we asymptotically expect to see the percolation critical behavior as the Griffiths phase is only present for $\theta > \theta_c$ in this case. In Ref. [7] it was found that the vicinity of the QMCP is highly anisotropic, as the ν correlation length critical exponent is different for the two control parameters, as listed in Table I. We have therefore also studied the behavior of the corner contribution to the entanglement entropy outside the critical point and measured $\mathcal{S}^{(d)}_{\rm cr}(L, \delta)$ as a function of either δ_θ or δ_p. In the upper panels of Fig. 4, $\mathcal{S}^{(d)}_{\rm cr}(L, \delta)$ is presented for box-h disorder in $d = 2$ for 10^4 samples, showing a clear peak at the QMCP in both directions. Outside the multicritical point, the corner contribution is limited by the finite correlation length, $\xi \sim |\delta|^{-\nu}$,

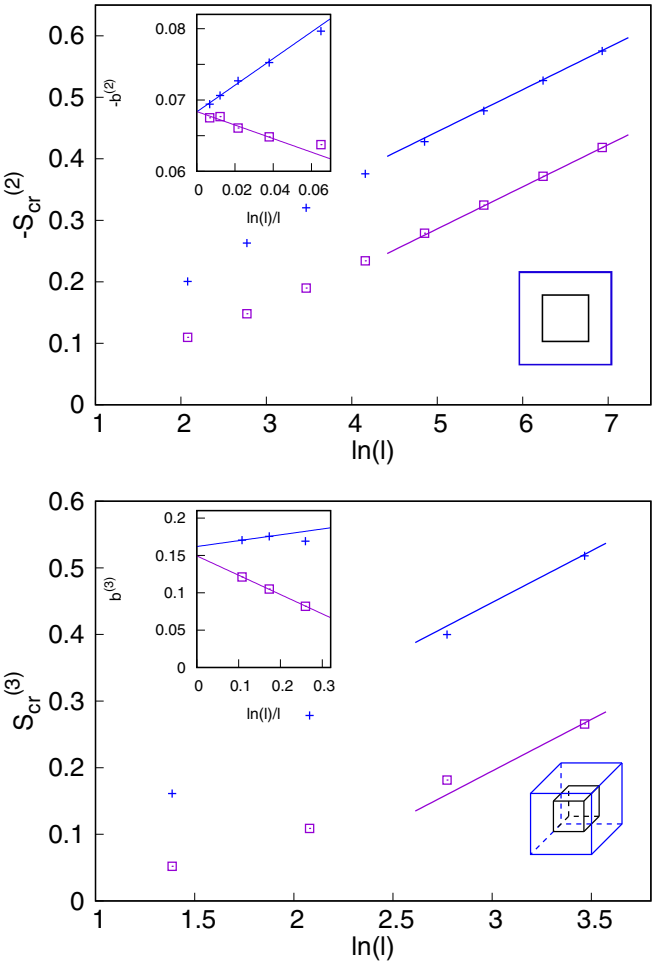

FIG. 3. Corner contribution to the entanglement entropy of cubic subsystems in the $d = 2$ (top) and $d = 3$ (bottom) models for fixed-h (+) and box-h (□) disorder realizations. Insets: Extrapolation of the effective prefactors of the logarithm are shown as calculated by two-point fits. As an indication of universality, the extrapolated values are disorder independent as listed in Table I. The error of the data points is smaller than the size of the symbols.

leading to the substitution $\ell \to \xi$. Therefore, close to the multicritical point, in the Griffiths phase, the corner contribution satisfies the scaling relation

$$\mathcal{S}_{\rm cr}^{(d)}(L,\delta) - b^{(d)} \ln L = f(\delta L^{1/\nu}), \tag{5}$$

as illustrated by the data collapse in the lower panels of Fig. 4. Here, we have used the known $d = 2$ estimates for the ν_p and ν_θ correlation length critical exponents, listed in Table I. These results underline that the corner contribution is not only universal, but provides a systematic way to locate the multicritical points in higher-dimensional interacting quantum systems, as well as b and the ν_θ and ν_p critical exponents. Let us emphasize again that the behavior of the corner term is in stark contrast to the full entanglement entropy, which is generally nonuniversal and nonmaximal at the critical point in higher dimensions.

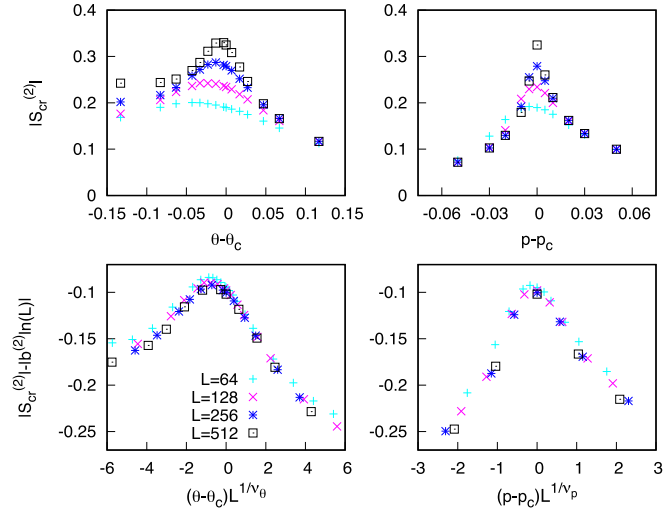

FIG. 4. Corner contribution to the entanglement entropy in the vicinity of the QMCP for box-h disorder in $d = 2$. Left: Varying θ at p_c (brown in Fig. 1). Right: Varying p at θ_c (green in Fig. 1). Bottom: Data collapse with the estimated value of $b^{(2)}$ as well as the known values of the ν_θ and ν_p critical exponents, listed in Table I. The error of the data points is smaller than the size of the symbols.

IV. DISCUSSION

We have studied the quantum entanglement properties at the multicritical point (QMCP) of a paradigmatic interacting quantum system (RTIM) in both two and three dimensions. While the area law is found to be valid for cubic subsystems, we have identified universal logarithmic corner contributions. The results at the QMCP are found to be between that of the two participating critical lines—corresponding to the percolation and generic QCPs—in both $d = 2$ and $d = 3$. This work contributes to the emerging picture of how universal features of entanglement manifest at higher-dimensional QCPs and QMCPs. For a single subsystem, geometric singularities, such as corners, play an essential role and lead to a universal prefactor b, akin to a critical exponent, which is independent from the usual set of exponents. In contrast to traditional critical exponents b aggregates higher-order correlations [35], and is expected to showcase a nontrivial dependence on the shape of the subsystem.

Measuring the shape dependence of the entanglement entropy at QCPs and at the QMCP is an interesting future direction, also related to recently proposed models of quantum communication [44]. For example, in $d = 2$ the shape dependence can be confronted with the results of conformal invariance. Currently, the most complete results are available at the percolation QCP, where in two dimensions the system is conformally invariant, enabling a full analytic treatment supported by high-precision numerical methods [36,43]. Detailed shape dependences of the cluster counts have been also obtained numerically for the percolation QCP in three dimensions [36,45]. In general, especially in the lack of conformal invariance, the shape dependence of the corner contributions is expected to be universal but nontrivial, meaning that different subsystem shapes might extract different information on the entanglement patterns. As the simplest possibility,

line segments of length ℓ are of special interest [36]. Line segments are special cases of *skeletal entanglement*, where the subsystem is a zero-measure volume of the full system, offering additional universal results [46].

Another key question that arises is whether studying multipartite entanglement can provide further insights [47,48]. As shown recently in the one-dimensional RTIM [49], the multipartite entanglement structure [50] is qualitatively different in otherwise similar disordered quantum chains [51]. The RTIM results also showed that in the appropriate geometric scaling limit, multipartite entanglement measures are universal and provide deeper information than bipartite entanglement. On the contrary to the entanglement entropy, where only the (leading order of the) corner contribution is universal, in the case of both the entanglement negativity and mutual information, the entire multipartite measure was found to be universal [49]. Extending these results to nonadjacent subsystems in higher-dimensional QCPs and QMCPs is an exciting future direction. Our results can be also extended to the RTIM with long-range interactions [52–54], motivated by materials such as $LiHo_xY_{1-x}F_4$ [37].

ACKNOWLEDGMENTS

This work was supported by the National Science Foundation under Grant No. PHY-2310706 of the QIS program in the Division of Physics.

[1] S. Sachdev, *Quantum Phase Transitions* (Cambridge University Press, Cambridge, UK, 1999).

[2] D. Belitz, T. R. Kirkpatrick, and T. Vojta, Nonanalytic behavior of the spin susceptibility in clean Fermi systems, Phys. Rev. B **55**, 9452 (1997).

[3] A. V. Chubukov, C. Pepin, and J. Rech, Instability of the quantum-critical point of itinerant ferromagnets, Phys. Rev. Lett. **92**, 147003 (2004).

[4] G. J. Conduit, A. G. Green, and B. D. Simons, Inhomogeneous phase formation on the border of itinerant ferromagnetism, Phys. Rev. Lett. **103**, 207201 (2009).

[5] C. J. Pedder, F. Krüger, and A. G. Green, Resummation of fluctuations near ferromagnetic quantum critical points, Phys. Rev. B **88**, 165109 (2013).

[6] S. Friedemann, W. Duncan, M. Hirschberger, T. Bauer, R. Küchler, A. Neubauer, M. Brando, C. Pfleiderer, and F. M. Grosche, Quantum tricritical points in $NbFe_2$, Nat. Phys. **14**, 62 (2018).

[7] I. A. Kovács, Quantum multicritical point in the two- and three-dimensional random transverse-field Ising model, Phys. Rev. Res. **4**, 013072 (2022).

[8] D. S. Fisher, Random transverse field Ising spin chains, Phys. Rev. Lett. **69**, 534 (1992); Critical behavior of random transverse-field Ising spin chains, Phys. Rev. B **51**, 6411 (1995).

[9] D. S. Fisher, Phase transitions and singularities in random quantum systems, Physica A **263**, 222 (1999).

[10] S. K. Ma, C. Dasgupta, and C.-K. Hu, Random antiferromagnetic chain, Phys. Rev. Lett. **43**, 1434 (1979); C. Dasgupta and S. K. Ma, Low-temperature properties of the random Heisenberg antiferromagnetic chain, Phys. Rev. B **22**, 1305 (1980).

[11] For reviews, see F. Iglói and C. Monthus, Strong disorder RG approach of random systems, Phys. Rep. **412**, 277 (2005); Strong disorder RG approach—a short review of recent developments, Eur. Phys. J. B **91**, 290 (2018).

[12] B. M. McCoy and T. T. Wu, Theory of a two-dimensional Ising model with random impurities. I. Thermodynamics, Phys. Rev. **176**, 631 (1968); Theory of a two-dimensional Ising model with random impurities. II. Spin correlation functions, **188**, 982 (1969); B. M. McCoy, Theory of a two-dimensional Ising model with random impurities. III. Boundary effects, *ibid.* **188**, 1014 (1969); Theory of a two-dimensional Ising model with random impurities. IV. Generalizations, Phys. Rev. B **2**, 2795 (1970).

[13] R. Shankar and G. Murthy, Nearest-neighbor frustrated random-bond model in $d = 2$: Some exact results, Phys. Rev. B **36**, 536 (1987).

[14] A. P. Young and H. Rieger, Numerical study of the random transverse-field Ising spin chain, Phys. Rev. B **53**, 8486 (1996).

[15] F. Iglói and H. Rieger, Density profiles in random quantum spin chains, Phys. Rev. Lett. **78**, 2473 (1997); Random transverse Ising spin chain and random walks, Phys. Rev. B **57**, 11404 (1998).

[16] P. Calabrese, J. Cardy, and B. Doyon, Entanglement entropy in extended quantum systems (special issue), J. Phys. A: Math. Theor. **42**, 500301 (2009).

[17] L. Amico, R. Fazio, A. Osterloh, and V. Vedral, Entanglement in many-body systems, Rev. Mod. Phys. **80**, 517 (2008).

[18] J. Eisert, M. Cramer, and M. B. Plenio, *Colloquium*: Area laws for the entanglement entropy, Rev. Mod. Phys. **82**, 277 (2010).

[19] N. Laflorencie, Scaling of entanglement entropy in the random singlet phase, Phys. Rev. B **72**, 140408(R) (2005).

[20] C. Holzhey, F. Larsen, and F. Wilczek, Geometric and renormalized entropy in conformal field theory, Nucl. Phys. B **424**, 443 (1994).

[21] G. Vidal, J. I. Latorre, E. Rico, and A. Kitaev, Entanglement in quantum critical phenomena, Phys. Rev. Lett. **90**, 227902 (2003).

[22] P. Calabrese and J. Cardy, Entanglement entropy and quantum field theory, J. Stat. Mech.: Theory Exp. (2004) P06002.

[23] L. Tagliacozzo, G. Evenbly, and G. Vidal, Boundary quantum critical phenomena with entanglement renormalization, Phys. Rev. B **80**, 235127 (2009).

[24] H. F. Song, N. Laflorencie, S. Rachel, and K. Le Hur, Bipartite fluctuations as a probe of many-body entanglement, Phys. Rev. B **83**, 224410 (2011); A. B. Kallin, M. B. Hastings, R. G. Melko, and R. R. P. Singh, Anomalies in the entanglement properties of the square-lattice Heisenberg model, *ibid.* **84**, 165134 (2011).

[25] D. S. Rokhsar and S. A. Kivelson, Superconductivity and the quantum hard-core dimer gas, Phys. Rev. Lett. **61**, 2376 (1988).

[26] E. Fradkin and J. E. Moore, Entanglement entropy of 2D conformal quantum critical points: Hearing the shape of a quantum drum, Phys. Rev. Lett. **97**, 050404 (2006); J.-M. Stéphan, S.

Furukawa, G. Misguich, and V. Pasquier, Shannon and entanglement entropies of one- and two-dimensional critical wave functions, Phys. Rev. B **80**, 184421 (2009); M. P. Zaletel, J. H. Bardarson, and J. E. Moore, Logarithmic terms in entanglement entropies of 2D quantum critical points and Shannon entropies of spin chains, Phys. Rev. Lett. **107**, 020402 (2011).

[27] G. Refael and J. E. Moore, Criticality and entanglement in random quantum systems, J. Phys. A: Math. Theor. **42**, 504010 (2009).

[28] I. A. Kovács and F. Iglói, Infinite-disorder scaling of random quantum magnets in three and higher dimensions, Phys. Rev. B **83**, 174207 (2011); Renormalization group study of random quantum magnets, J. Phys.: Condens. Matter **23**, 404204 (2011).

[29] O. Motrunich, S.-C. Mau, D. A. Huse, and D. S. Fisher, Infinite-randomness quantum Ising critical fixed points, Phys. Rev. B **61**, 1160 (2000).

[30] Y.-C. Lin, N. Kawashima, F. Iglói, and H. Rieger, Numerical renormalization group study of random transverse Ising models in one and two space dimensions, Prog. Theor. Phys. Suppl. **138**, 479 (2000).

[31] D. Karevski, Y.-C. Lin, H. Rieger, N. Kawashima, and F. Iglói, Random quantum magnets with broad disorder distribution, Eur. Phys. J. B **20**, 267 (2001).

[32] Y.-C. Lin, F. Iglói, and H. Rieger, Entanglement entropy at infinite-randomness fixed points in higher dimensions, Phys. Rev. Lett. **99**, 147202 (2007).

[33] R. Yu, H. Saleur, and S. Haas, Entanglement entropy in the two-dimensional random transverse field Ising model, Phys. Rev. B **77**, 140402(R) (2008).

[34] I. A. Kovács and F. Iglói, Critical behavior and entanglement of the random transverse-field Ising model between one and two dimensions, Phys. Rev. B **80**, 214416 (2009); Renormalization group study of the two-dimensional random transverse-field Ising model, **82**, 054437 (2010).

[35] I. A. Kovács and F. Iglói, Universal logarithmic terms in the entanglement entropy of $2d$, $3d$ and $4d$ random transverse-field Ising models, Europhys. Lett. **97**, 67009 (2012).

[36] H. S. Ansell, S. J. Frank, and I. A. Kovács, Cluster tomography in percolation, Phys. Rev. Res. **5**, 043218 (2023).

[37] D. M. Silevitch and G. Aeppli, and T. F. Rosenbaum, Switchable hardening of a ferromagnet at fixed temperature, Proc. Natl. Acad. Sci. USA **107**, 2797 (2010).

[38] A. B. Harris, Effect of random defects on the critical behaviour of Ising models, J. Phys. C: Solid State Phys. **7**, 3082 (1974); R. B. Stinchcombe, Ising model in a transverse field. I. Basic theory, *ibid.* **14**, L263 (1981); R. R. dos Santos, The pure and diluted quantum transverse Ising model, *ibid.* **15**, 3141 (1982).

[39] T. Senthil and S. Sachdev, Higher dimensional realizations of activated dynamic scaling at random quantum transitions, Phys. Rev. Lett. **77**, 5292 (1996).

[40] I. A. Kovács and R. Juhász, Emergence of disconnected clusters in heterogeneous complex systems, Sci. Rep. **10**, 21874 (2020).

[41] G. Refael and J. E. Moore, Entanglement entropy of random quantum critical points in one dimension, Phys. Rev. Lett. **93**, 260602 (2004).

[42] I. A. Kovács and F. Iglói, Corner contribution to percolation cluster numbers in three dimensions, Phys. Rev. B **89**, 174202 (2014).

[43] I. A. Kovács, F. Iglói, and J. Cardy, Corner contribution to percolation cluster numbers, Phys. Rev. B **86**, 214203 (2012).

[44] R. T. C. Chepuri and I. A. Kovács, Complex quantum network models from spin clusters, Commun. Phys. **6**, 271 (2023).

[45] J. Wang, Z. Zhou, W. Zhang, T. M. Garoni, and Y. Deng, Bond and site percolation in three dimensions, Phys. Rev. E **87**, 052107 (2013).

[46] C. Berthiere and W. Witczak-Krempa, Entanglement of skeletal regions, Phys. Rev. Lett. **128**, 240502 (2022).

[47] Sz. Szalay, Multipartite entanglement measures, Phys. Rev. A **92**, 042329 (2015).

[48] V. Eisler and Z. Zimborás, Entanglement negativity in two-dimensional free lattice models, Phys. Rev. B **93**, 115148 (2016).

[49] J. S. Zou, H. S. Ansell, and I. A. Kovács, Multipartite entanglement in the random Ising chain, Phys. Rev. B **106**, 054201 (2022).

[50] P. Ruggiero, V. Alba, and P. Calabrese, The entanglement negativity in random spin chains, Phys. Rev. B **94**, 035152 (2016).

[51] F. Iglói and R. Juhász, Exact relationship between the entanglement entropies of XY and quantum Ising chains, Europhys. Lett. **81**, 57003 (2008).

[52] R. Juhász, I. A. Kovács, and F. Iglói, Random transverse-field Ising chain with long-range interactions, Europhys. Lett. **107**, 47008 (2014).

[53] R. Juhász, I. A. Kovács, and F. Iglói, Long-range epidemic spreading in a random environment, Phys. Rev. E **91**, 032815 (2015).

[54] I. A. Kovács, R. Juhász, and F. Iglói, Long-range random transverse-field Ising model in three dimensions, Phys. Rev. B **93**, 184203 (2016).